Injectable therapeutic organoids using sacrificial hydrogels

Ninna S. Rossen,[1,2,3]† Priya N. Anandakumaran,[1]† Rafael zur Nieden,[1]† Kahmun Lo,[1] Wenjie Luo,[1] Christian Park,[1] Chuqiao Huyan,[1] Qinyuouen Fu,[1] Ziwei Song,[1] Rajinder P. Singh-Moon,[1] Janice Chung,[1] Jennifer Goldenberg,[1] Nirali Sampat,[1] Tetsuhiro Harimoto,[1] Danielle Bajakian,[4] Brian M. Gillette,[1] and Samuel K. Sia[1]*

[1]Department of Biomedical Engineering, Columbia University, 351 Engineering Terrace, 1210 Amsterdam Avenue, New York, NY, USA 10027.

[2]Biotech Research & Innovation Centre, University of Copenhagen, University of Copenhagen, Ole Maaløes Vej 5, 2200 Copenhagen N, Denmark (Current affiliation)

[3]Department of Radiation Oncology, Stanford University, Palo Alto, CA, USA (Current affiliation)

[4]Department of Surgery - Division of Vascular Surgery and Endovascular Interventions, Columbia University Medical Center, Herbert Irving Pavilion, 161 Fort Washington Avenue, New York, NY, USA 10032.

† These authors made equal contributions.

*Correspondence to be addressed to ss2735@columbia.edu

Abstract

Organoids, by promoting self-organization of cells into native-like structures, are becoming widespread in drug-screening technologies, but have so far been used sparingly for cell therapy as current approaches for producing self-organized cell clusters lack scalability or reproducibility in size and cellular organization. We introduce a method of using hydrogels as sacrificial scaffolds, which allow cells to form self-organized clusters followed by gentle release, resulting in highly reproducible multicellular structures on a large scale. We demonstrated this strategy for endothelial cells and mesenchymal stem cells to self-organize into blood-vessel units, which were injected into mice using hypodermic needles, and observed in real time to rapidly form perfusing vasculature. As cell therapy transforms into a new class of therapeutic modality, this simple method – by making use of the dynamic nature of hydrogels – could offer high yields of self-organized multicellular aggregates with reproducible sizes and cellular architectures.

Introduction

Organoids, such as vascularized organoids or spheroids [1-3], are three-dimensional multicellular clusters which mimic the structure and function of native tissues and are useful for on-chip drug screening [4,5]. For use as a cell therapy, delivery of cells within well-controlled microenvironments, rather than suspensions of isolated cells, could promote and maintain desired cellular functions within dynamic and complex *in vivo* environments [6-11]. As organoids are increasingly being explored for *in vivo* studies and therapy, there is increasing recognition of the unmet challenge in generating multicellular aggregates with high reproducibility and control. As one example, even though control over "organoid size, shape, cellular composition and 3D architecture...is essential in order to understand the mechanisms that underlie organoid development in normal and pathological situations, and to use them as targets for manipulation or drug testing", reproducibility has been cited as "the major bottleneck of current organoid systems" [12].

The major current methods for generating organoids include spinner cultures [13], hanging drops [14,15], and non-adhesive 96-well plates [16-19] (Supplementary Table 1), but these methods are difficult to scale or harsh to cells. (Alternatively, microtissues that are "cells in gels" [20-23] typically feature cells moving to pre-formed pores within a hydrogel scaffold, but the cells are limited in their ability to self-organize into desired structures [24], and the resultant gels exhibit variable structures and sizes dependent on the pores and may be undesired in the implanted site due to potential immunogenicity). More recently, methods to fabricate organoids based on micro-sized wells have faced challenges of either high adsorption (of steroid hormones, small molecules, and drugs [25,26] for PDMS-based wells) or inefficient and

harsh processes, usually involving vigorous pipetting or high-speed centrifugation, to separate and remove the cellular clusters from the microwells. Such procedures produce cellular clusters at a low yield and could damage cellular structures and function. Recognizing this limitation, other studies have proposed more complex methods to actively release cellular clusters from microwells [27-29]. As such, there still lacks reliable methods to generate organoids at high yield and with reproducibility and control over aggregate size and cellular organization.

Many hydrogels are biocompatible and have been used as a dynamically responsive biomaterial (such as microfluidic valve [30], changing cellular microenvironment [31], and stimuli-responsive drug release [32]). We hypothesize that a dynamic change in the cross-linking state of hydrogels could gently release organoids, and sought to demonstrate the strategy for producing large numbers of vascularized organoids with high reproducibility and scalability, as well as the ability to retain functionality after passing through needles to obviate invasive surgery [33,34]. We also assessed the ability of the pre-formed blood-vessel units, after injection, to rapidly integrate with the host's vascular network in a healthy mouse model.

Results

Hydrogels as a sacrificial scaffold as a gentle and scalable method for producing and harvesting organoids

Sacrificial materials are widely used in micromachining of microelectromechanical systems (MEMS) to release patterned metals or semiconductors from a substrate (Figure 1a).

To cellular structures, some hydrogels (such as agarose or poly(ethylene)glycol as previously demonstrated) can be non-adhesive and thereby promote cells to interact with one another and contract into microtissues and organoids [1,35]. We hypothesized that a dynamic change in the cross-linking state of alginate, which can be achieved by adding calcium or a chelator and has been demonstrated for other purposes [31,36]. could similarly release cell-based structures from a surface without significantly disrupting the organoid structures or underlying cell function [37,38]. Specifically, we deposit the sacrificial material, create the sacrificial structure by cross-linking the alginate in its patterned state, deposit cells on top to allow cellular self-organization to take place, and remove the sacrificial layer by adding a chelator (5% w/v sodium citrate) (Fig. 1a; see Supplementary Figure 1 for fabrication details). The alginate is uncrosslinked within ~12 minutes (Fig. 1b), to gently release a large number of organoids floating in solution (Fig. 1c,d; Supplementary Video 1). The resulting organoid solution could be gently pipetted into tubes, centrifuged and resuspended in a culture medium suitable for downstream manipulation or direct cell delivery. Each step is simple, can be conducted with sterile liquid handling, and can be automated.

The step of cellular self-organization can be adjusted depending on the organoid of interest. For vascularized organoids (Fig. 1c), we seeded a co-culture containing ECs and MSCs (of either mouse or human origin) into the dissolvable alginate microwells. We cultured the cells in media without growth factors ("maintenance" medium), followed by a vasculogenic medium with growth factors to induce cell-cell interactions including sprouting of blood vessel-like structures. The organoids, now containing blood vessel-like structures, contract and are gently released by dissolving the alginate microwells.

The same small number of steps (Fig. 1c, d) can harvest a large number of organoids by using alginate templates with large numbers of microwells. As an example, we demonstrated three different sizes of alginate microwell inserts for culture dishes (Fig. 2a): 15.6 mm-diameter inserts containing >1000 microwells (yielding >24,000 organoids on a 24-well plate), 22.1-mm inserts containing >3000 microwells (yielding >36,000 organoids on a 12-well plate), and a 60-mm diameter insert containing >30,000 microwells in a 60-mm culture dish. If desired, the inserts can be stacked to increase the number of organoids produced in the same area with additional media changes.

We demonstrated this massive parallel production of more than 30,000 organoids by seeding a quarter of a billion cells (Fig. 2b) in one 60-mm dish insert (Fig. 2c). We also tested the ability of the organoids to assemble *in vitro* into a microvascular network (Fig. 2d). We co-cultured RFP-labelled MSCs and GFP-labelled ECs for four days, gently harvested the organoids, and assembled them into a macroscopic tissue with surface area of 1 cm^2 and a height of 1 mm (Fig. 2d). We performed fluorescence imaging of this macroscopic tissue (Fig. 2e). The organoids were densely packed, and exhibited distinct endothelial core structures, confirming that the gentle harvest and assembly did not disturb the internal architecture of the organoids. The assembled macrotissue, consisting of fully contracted organoids, did not visibly contract during subsequent *in vitro* culture.

Production of organoids with reproducible size and structure

Next, we studied whether the sizes and internal architectures of organoids could be controlled reproducibly. In the absence of exogenous growth factors, we observed that GFP-labelled human umbilical vein endothelial cells (HUVECs), which were initially randomly

distributed alongside RFP-labelled mouse MSCs, migrate to the center of the organoids and form endothelial cores after culture in the "maintenance" medium for 3 days (Fig. 3a, top panel, and Supplementary Video 2). Similarly, ECs also formed endothelial cores when co-cultured with another cell type (fibroblasts) in a medium without growth factors (Supplementary Figure 2), the endothelial cores were more pronounced than in a previous observation [19]. By contrast, ECs did not migrate to the center when the organoids were initially cultured in a vasculogenic medium containing 50 ng/mL VEGF and 50 ng/mL bFGF (Fig. 3a, bottom panel), consistent with a previous observation [9]. Overall, the data showed the organoids to exhibit reproducible internal architectures containing endothelial cores.

We characterized the reproducibility of the method in controlling the size of the pre-vascularized organoid. By varying the microwell sizes and the co-culture ratios of cell types (Fig. 3b), we controlled the number of cells that could aggregate into a single organoid. For example, microwells of three different sizes (100, 200, and 400 μm diameter) yielded organoids of three different sizes (39±3 μm, 71±5 μm, and 82±7 μm diameter, respectively, all at the same cell-seeding concentration) (Fig. 3b). The well size was chosen to be large enough to hold all the cells at the initial seeding concentration, but small enough to ensure sufficient cell-cell contact to form a single organoid rather than multiple organoids. The cells aggregated into compact organoids within the first two days of *in vitro* culture, as seen by the decreasing radius of the smallest circle to include all cells (Fig. 3c), with the main contraction happening in the first day and no further contraction after three days. We also observed that the size of the fully contracted organoids (at day 2 and after) correlated to the number of cells in the organoid as expected; the diameter of the organoids' cross sections related to the number of cells in the organoid and the cells typical volume as $r_{organoid} = (6/\pi\, v_{cell}\, n_{cell})^{1/3}/2$ (Supplementary Figure 3).

Also, we quantitatively analyzed the formation of organoids for cultures containing only MSCs, and co-cultures with EC:MSC ratios of 1:3, 1:1, and 3:1 (Fig. 3b-e). In 200-μm microwells, over three days, cells contracted into an organoid and ECs migrated towards the center (Fig. 3c), and co-cultures in 400 μm microwells showed similar trends in organoid contraction and EC migration (Supplementary Figure 4). Co-cultures in 100-μm microwells, however, did not contain enough cells (fewer than 150 cells in total) to form a distinct center (Supplementary Figure 5). We also observed that the organoids per unit area and the number of organoids containing defined internal architectures could be controlled by varying microwell sizes and ratios of cell types (Fig. 3e). (In subsequent *in vivo* studies, we have used 200-μm microwells with ratios of MSC only, 1 EC:3 MSC and 1 EC:1 MSC, as these conditions showed aggregation involving almost all the cells within the microwells.) Overall, the data showed the method can produce organoids with internal architectures at high throughput and different sizes controllably.

Production of pre-vascularized human organoids with reproducible size and structure

We examined the effectiveness of this method for producing pre-vascularized organoids containing human adipose-derived MSCs (hAMSCs) with human umbilical vein endothelial cells (HUVECs), in ratios of MSCs only, 1 EC:3 MSC, and 1 EC:1 MSC. We examined the maturation of organoids over 8 days, where organoids were first grown in maintenance medium over 3 days to form endothelial cores, and then switched to vasculogenic medium containing exogenous growth factors for 5 days (Fig. 4a). By day 8, vessel-like structures, such as lumens within the center of the organoid, with sprouting and maturation of vessels towards the surface were observed (especially evident in the larger

organoids of the 400-μm wells). The initial migration of ECs was apparent after 20 hours (Fig. 4b and Supplementary Figure 6). In addition, we placed multiple pre-vascularized organoids inside 400 μm alginate wells that were collagen-doped, to mimic the adhesiveness of native tissues. Within 24 hours, organoids attached to each other and contracted to form a larger, compact mesotissue (aggregation of multiple organoids) with a smooth outer border (Fig. 4c, with additional time points in Supplementary Figure 7 and Supplementary Video 3). Hence, this method produced organoids containing human ECs and MSCs, with control over sizes and spatial architectures, and confirming the ability to form a pre-vascularized mesotissue.

Rapid host perfusion of pre-vascularized organoids in mouse model

Next, we assessed the effectiveness of the prevascularized organoids to self-organize to form a vascular network, anastomose to native host vasculature, and be perfused with host blood in a mouse model (Fig. 5a). To facilitate real-time visualization, we performed surgery to place a window chamber (Supplementary Figure 8) to permit brightfield, epifluorescence and confocal imaging. We used organoids formed in 200-μm wells yielding organoids approximately 70 μm in diameter, which is also within the diffusion limit of oxygen [39]. We produced and harvested pre-vascularized organoids made of human cells (HUVECs and hAMSCs), which we injected into SCID mice, a well-established animal model for studying integration of xenografts made of human cells [40]. We could inject and monitor the vascular formation for multiple different conditions (e.g. 1 HUVEC : 1 hAMSC and hAMSC only) in the same mouse, by utilizing the strong bond between the fascia and the subdermis. We injected the organoids through the fascia and into the space between the fascia and the subdermis, leaving the subcutaneous tissue intact between injection sites to create a barrier

(Fig. 5b). The organoids held up intact to the shear stress of injection through a syringe and needle (Supplementary Figure 9). Interestingly, the shell of MSCs shielded the central blood-vessel building block against shear, and preserved the organoids' architectural integrity after they passed through the needle. (We also demonstrated the organoids could be injected directly into adipose tissue (Supplementary Figure 10) with good integration.)

We followed the formation of new vasculature by taking epiflourescent and stereoscopic images through the window chamber. Stereoscopic imaging (for example, of the 1 HUVEC : 1 hAMSC conditions) showed vessel formation between day 4 and 7 (Fig. 5b, top rows), with the implanted vasculature connected to the host vasculature and becoming perfused (Fig. 5b, top rows). After just 7 days, host perfusion of the implanted vasculature was prominent and intense. The vessels were functional for the remaining 16 days of the 23-day *in vivo* studies. Quantitatively, we measured the total length of perfused vasculature in three regions-of-interest (ROIs) within the area of injected organoids (Fig. 5c). At day 7, areas injected with pre-vascularized organoids showed significant formation of new perfused vasculature, while areas injected with organoids consisting of MSCs only showed no increase in perfused vasculature (Figs. 5b bottom row and 5c). For all four mice tested (each with multiple conditions in the window chamber), all conditions with EC-containing organoids showed rapid vascularization of the injected organoids.

We also explored whether this self-organizing, "micro-to-macro" strategy could provide a limited but reproducible level of architectural control in the overall branching length of implanted, perfused microvasculature. Specifically, we hypothesized that average distances between endothelial cores could be related to diameters of organoids. The mean length of the perfused branches for 1 EC:1 MSC at day 7 was 93±39 μm, with minimal

changes by day 9 to 11, when the mean branch length was 86±29 μm and 93±44 μm, respectively (Fig. 5d). Indeed, the length of the newly formed vasculature's branches reflected core-to-core distances between the densely packed, injected organoids with diameters of 71±5 μm.

We also used epiflourescence and confocal microscopy to characterize the formation and integration of the new vasculature. Observing the GFP-labeled HUVECs through the window chamber (Fig. 5e), we noticed the endothelial cores connecting with each other over time: the ECs initially appeared as discrete cores (day 0), then sprouted toward neighboring cores (day 4), connected with the host vasculature and became perfused (day 7), and stabilized as the perfused vascular network matured (day 9, 12, and 23). Between days 4 and 7, the network matured to form lumens (Fig. 5e, red arrows). (We further confirmed the lumenous structure of the newly-formed, perfused network on day 11 via confocal microscopy on day 11, Supplementary Video 4.) Moreover, we observed that areas indicating newly formed lumens (consisting of GFP-labelled HUVECs) co-localized with areas indicating host blood perfusion, further confirming that it was the newly-formed lumenous vasculature that was perfused, rather than angiogenesis from the host into the implanted tissue.

Discussion

Using sacrificial hydrogels to produce organoids with high reproducibility and scalability. Like the development of micromachining techniques for producing MEMS structures reproducibly and on a large scale, we have developed a technique to use sacrificial hydrogels to produce clusters of self-organized cell-based structures with high reproducibility

and scalability. Previously, we and other groups have shown the use of microfabricated hydrogels, including sacrificial techniques, to form *in vitro* microvascular networks [31,37,41,42]. This paper demonstrated the dynamic structure of hydrogels can also be exploited to produce and gently release organoids for cell therapy.

For purposes of cell therapy, it is critical for clinical efficacy, process control, and regulatory approval that cells introduced into the body are generated via tightly controlled processes and exhibit reproducible origin, size, and structure. Previous studies have observed that a "lack of control over the process is likely to underpin the variability in systems and experiments that, with few exceptions, does not allow [organoids] to yield their full potential", and the importance of achieving reproducible "organoid size, shape, cellular composition and 3D architecture" in future research on organoids as well as use for therapeutic purposes [12]. Compared to current organoid systems, our method can generate self-organized multicellular aggregates with both high yield (Supplementary Table 1) and high reproducibility over aggregate size and cellular organization (Supplementary Table 2). Moreover, the aggregate size and features of cellular organization can be tuned (Supplementary Table 2), as our method bears similarities to MEMS fabrication technologies (in contrast to "cells in gels" systems which feature a distribution of pore sizes). In this study, sizes and internal architectures of the organoids were reproducible for different types of cells (MSCs and ECs of mouse and human origin), cell ratios, and overall size of microwells which determined the diameter of the contracted organoids. Even at the tissue level both *in vitro* and *in vivo*, branching lengths of the vascular network were reproducible (by contrast, microtissues with ECs had previously yielded non-uniform branching lengths [7,16,43].)

Also, an ideal method for generating organoids should be scalable and gentle. In the common hanging-drop method, 384 organoids could be produced in the area of an overall standard well plate (with the overall scalability limited by the number of wells [14]), whereas the smallest construct shown in Fig. 2 produces 24,000 organoids in the same area with fewer steps needed (e.g. media-changing steps, one alginate dissolving step), all of which could be automated by liquid handling. The release of organoids is gentle even at a large scale, in contrast to vigorous pipetting or high-speed centrifugation for current microwell procedures. For cell therapy, it is important that the integrity of the cells be preserved (for example, a FDA guidance document points to the need "to preserve integrity and function so that the products will work as they are intended" [44]. Beyond cell therapy, large-scale and effective production of organoids (beyond the quarter billion cells demonstrated) could also support studies in developmental biology, cancer cell intravasation [16], and organ printing.

An advanced, controlled form of cell therapy. In past studies, needle injection (and organ printing) with unilaminar vascular organoids [45,46] had been challenging due to shear stress formation. It would be advantageous in cell therapy to be able to deliver the cells via minimally invasive injection rather than invasive surgery. Our method produced organoids which held up intact to shear stress during injections, even with high (25 to 30)-gauge needles (Supplementary Figure 9). This behavior may partially have been due to a shell of MSCs which protected the endothelial structure; interestingly, previous studies have also shown that the MSCs could act as an immune-suppressive shield for cell therapy in addition to providing angiogenic signaling [47,48].

A potential application of these organoids is to treat peripheral artery disease, the most severe form of which is critical limb ischemia (CLI) which can lead to amputations [49].

315 To date, over 50 cell-therapy trials are at clinical stages for treating CLI. Many trials involve
316 injecting MSCs [49-53] or ECs (such as MarrowStim)[52,54,55], but the cells could die from
317 deprivation of oxygen and nutrients before they are able to assemble into vascular networks
318 *in vivo* and anastomose with host vasculature. The use of therapeutic pre-vascularized
319 organoids could overcome many of the issues associated with currently cell therapy trials in
320 clinical trials to treat CLI. In a clinical scenario, such an approach could be especially
321 attractive for "no-option" patients on the verge of amputation with subsequently poor
322 mortality outcomes (60% within five years of surgery [49]).
323

MATERIALS AND METHODS

Experimental design

The objective of this study was to develop an approach to form self-organized organoids in a scaleable and gentle manner, for use as an injectable cell therapy. As such, we designed dissolvable alginate microwells to culture organoids, promote self-organization of the cells, and gently harvest the organoids. We then demonstrated their functionality in a healthy mouse model using a window chamber assay. All cells used in these studies were purchased commercially, all animal procedures were approved by the Columbia University Institutional Animal Care and Use Committee (IACUC) and all experiments were performed in accordance with relevant guidelines/regulations.

Fabrication of alginate microwells

We developed an experimental setup to culture cellular organoids with high throughput and without the labor-intensive hanging drop approach. We seed the cells onto an alginate construct with between 379 and 30,000 microwells. The cells will settle into these microwells, and as the alginate provides no adherence structure for the cells, the cells will adhere strongly to each other forming spherical cell aggregates over the initial 24 hours.

The alginate microwells are cast on hydrophilic PDMS molds. We fabricated master molds in SU-8 (SU-8 3050, Microchem, Newton, MA) on 3-inch Si wafers (Silicon Sense, Nashua, NH) by photolithography as described before [38] to cast polydimethylsiloxane (PDMS, Sylgard 184, Essex Brownell, Fort Wayne, IN) replicas from the masters. We then made the PDMS molds hydrophilic by plasma treatment, and submerged them in distilled water to retain their hydrophilicity. We then autoclaved the PDMS molds prior to casting alginate.

We then prepared and autoclaved a 2% w/v alginate (Pronova UltraPure MVG, NovaMatrix, Drammen, Norway) or 7.5% w/v alginate (Alginic acid sodium salt, Millipore Sigma, St Louis, MO) in HEPES saline buffer solution (Ultrasaline A, Lonza, Basel, Switzerland). The alginate was pipetted into the PDMS molds. We used positive-displacement pipettes for accurate pipetting of viscous alginate solutions and to avoid bubbles. We closed the top of the molds with cellulose dialysis membranes (6000 Da MWCO), and flattened the membranes using the edge of a sterile glass slide. A 60 mM $CaCl_2$ HEPES buffer solution was pipetted on top of the membrane for at least 60 min to crosslink the alginate at room temperature. We removed the hydrogels from the molds using sterilized tools, and placed the hydrogels in HEPES saline buffer solution (Ultrasaline A, Lonza, Basel, Switzerland) supplemented with 1.8 mM $CaCl_2$ (to prevent leaching of the calcium ions from the hydrogels). We then transferred the alginate hydrogels into sterile culture ware, such as 24-well plates (Fisher Scientific, Fair Lawn, NJ) with the open micro wells facing up and stored them at 4°C until further use.

Uncrosslinking of sacrificial alginate

To determine the length of time required to uncrosslink the microwells, 7.5% w/v alginate microwells were fabricated as described in the previous section, and stored in 1.8mM $CaCl_2$ overnight. The following day, the alginate microwell scaffolds were transferred to preweighed, individually cut wells (from a 24 well plate), any excess $CaCl_2$ was removed, and the initial mass of the alginate scaffolds was measured. We then added 1 mL of PBS, 0.5% w/v sodium citrate, or 5% w/v sodium citrate to the well, and after 1 minute the excess supernatant was removed, the remaining alginate scaffold was weighed, and a fresh solution of PBS, 0.5% sodium citrate or 5% sodium citrate was added. This was repeated until the alginate microwell scaffold was fully uncrosslinked (by the sodium citrate).

374

375 **Cell sources**

376 GFP-labeled human umbilical vein endothelial cells (GFP-hUVECs)
377 (Angioproteomie, MA, USA) were cultured in Endothelial Growth Medium 2 (PromoCell,
378 Heidelberg, Germany). Adipose derived human mesenchymal stem cells (hAMSCs)
379 (Promocell, Heidelberg, Germany) were cultured in Mesenchymal Stem Cell Growth
380 Medium (Promocell, Heidelberg, Germany). RFP-labeled mouse mesenchymal stem cells
381 (RFP-mMSCs) (Cyagen, CA, USA) were cultured in DMEM with 10% FBS and 1%
382 PenStrep (all from LifeTechnologies). All cells were gently passaged at 80-90% confluency
383 using TrypLE (LifeTechnologies) and used only until passage P6 and mMSC until P8. Cells
384 were cultured in 37°C and 5% CO_2-balanced, humidified atmosphere.

385

386 **Fabrication of organoids**

387 HUVECs and MSCs were harvested from 2D cell culture, counted and desired cell
388 ratios of HUVECs to MSCs were prepared: MSC only, 1 HUVEC to 3 MSC, 1 HUVEC to 1
389 MSC and 3 HUVEC to 1 MSC.

390 Then the 1.8 mM $CaCl_2$ solution that the alginate microwells were stored in was
391 removed, and replaced with DMEM (ATCC, Manassas, VA). The microwells were then
392 placed in the incubator at 37°C and 5% CO_2 to equilibrate for at least 20 minutes. Then
393 DMEM was removed and the microwell constructs gently dried using surgical spears
394 (Braintree Scientific, Braintree, MA) leaving the microwell features covered.

395 Cell suspensions were then pipetted on to alginate molds of 100, 200 and 400 μm
396 microwell size using a positive displacement pipette. Cells were left to settle to the bottom of
397 the microwells for 20 minutes and the culture wells were then filled up with culture medium.

398

399 **Culture media**

400 The first 3-4 days after seeding, the cells were cultured in maintenance medium:
401 Dulbecco's Modified Eagle Medium (DMEM) with 10% Fetal Bovine Serum (FBS) and 1%
402 PenStrep (all from LifeTechnologies), with 50 μg/mL Sodium L-ascorbate (Sigma-Aldrich).
403 For Fig. 4 and 5, the maintenance medium also included 20 mM Hepes (Fisher Scientific,
404 Fair Lawn, NJ), 1 μM Insulin (LifeTechnologies, Carlsbad, CA), 250 nM T3, 1 μM
405 dexamethasone, 0.5 mM IBMX, 50 μM Indomethacine, 1 μM Rosiglitazone and 1 μM
406 CL316243 (all from Sigma, St. Louis, MO). After the first 3-4 days, the media was changed
407 from maintenance medium to vasculogenic medium: Dulbecco's Modified Eagle Medium
408 (DMEM) with 10% Fetal Bovine Serum (FBS) and 1% PenStrep (all from
409 LifeTechnologies), with 50 μg/mL Sodium L-ascorbate (Sigma-Aldrich), 40 ng/mL bFGF
410 and 40 ng/mL VEGF recombinant human protein (both from LifeTechnologies). For Fig. 4
411 and 5, the vasculogenic media also included 20 mM Hepes, 1 μM Insulin, and 250 nM T3.
412 The cells were cultured in vasculogenic medium up to day 11. Cell media was changed every
413 other day.
414
415 **Harvesting of organoids**

416 To collect organoids, the alginate hydrogel was uncrosslinked [37]. For this, the culture
417 medium of the organoids was replaced with 5%w/v sodium citrate solution for approximately
418 20 min. This chelator liquefied the alginate, and allowed for resuspension of the organoids in
419 a desired medium. Organoids were then centrifuged at 300 rpm for 5 minutes or as specified
420 and the organoid pellet carefully collected for further use.
421
422 **Organoid fusion**

To test the ability of organoids to assemble *in vitro* and fuse to a larger tissue, 200 μm sized organoids of only hAMSCs, 1 EC : 3 hAMSC and 1 EC : 1 hAMSC ratio were placed in a 400 μm sized microwell of collagen-doped alginate [38] composed of 3.5% collagen and 1% alginate. These organoids had previously been prevascularized as described above. Organoid fusion was conducted in vasculogenic medium and observed for 24 hours.

Formation of macrotissue

To yield a large enough number of organoids in parallel to produce a macroscopic tissue, we seeded a co-culture of 1 MSC : 1 EC ratio onto an alginate microwell construct that fits into a 60 mm culture dish and produces over 30,000 organoids (Fig. 2a and c). The cells were cultured in maintenance medium without growth factors for 4 days with daily media change due to the high number of cells. The organoids were collected by removing the medium and uncrosslinking the alginate with 5 mL 5%w/v sodium citrate solution. The alginate liquefied and the organoid solution was gently collected, spun down and resuspended in 1 mL vasculogenic media. To facilitate sustained culture and imaging of the macro-tissue, we had constructed a 1 cm^2 cylindrical hole in a 1 cm thick 10% agarose layer in the middle of a 60 mm dish. The hole was made by placing a 1 cm^2 by 1 cm PDMS mold in the middle, pouring on agarose and removing the PDMS cylinder when the agarose had gelled. The 1 mL organoid suspension was pipetted into the hole, allowed to settle for 1 hour, and then had 5 mL vasculogenic media added on top. The media was changed daily.

Window chamber surgery

Organoids were collected as described above. The suspension was gently spun down at 220 g for 5 minutes. The supernatant was removed and the organoids resuspended in 200 μl PBS. In vitro created, prevascularized and non-prevascularized organoids were implanted in a

window chamber to allow for continuous in vivo monitoring of the vascularization and integration process. Window chamber surgeries were conducted as described previously [56,57]. A titanium window chamber (APJ Trading, Ventura, CA) was surgically implanted midline on the dorsum of male SCID mice (strain: ICRSC-M-M, 5-6 weeks of age, Taconic, Hudson, NY) after hair removal and ethanol and iodine disinfection.

To reduce variability between mice, prevascularized and non-prevascularized organoids were implanted in individual compartments of the same window chamber. Organoids were delivered by injection and pipetting underneath the fascia of connective tissue to the subcutaneous adipose tissue. Window chambers were closed with a circular glass cover slip and a retaining ring (APJ Trading, Ventura, CA). A custom-made 3D printed window chamber backing was attached to reduce skin movement in the window chamber. In a subset of experiments, a custom-made ultem plastic 9 well array was screwed onto the front frame of the window chamber to allow for high throughput in vivo testing. Here, organoids were placed into one of the 9 wells.

Animals were housed aseptically in frog cages to allow for enough clearance for the window chamber while still permitting easy access to standard laboratory chow (Irradiated globle rodent diet, Fisher Scientific, Fair Lawn, NJ) and drinking water ad libitum. Follow up buprenorphine administration (0.1mg/kg bodyweight) for pain management was given subcutaneously every 6-12 hours after surgery for the next 2 days post-OP. CO_2 euthanasia and cervical dislocation were performed after 30 days or earlier if necessary.

The animal procedures were approved and carried out in accordance to local regulations and authorities. The surgeries were conducted in aseptic technique.

Imaging

A Leica DMI 6000B inverted microscope with 4x and 10x objectives, equipped with a motorized stage (Leica Microsystems, Bannockburn, IL) and a QImaging Retiga 2000R

473 monochrome camera (QImaging, Surrey BC, Canada) was used to acquire fluorescence and
474 brightfield images. Leica LAS X software was used for image acquisition. Cropping, color
475 adjustments and contrast enhancements of images as well as Z-stack projections were
476 performed in ImageJ. For time lapse imaging of organoid formation and organoid fusion an
477 environmental chamber was used to maintain 37°C and 5% CO_2. Images were acquired
478 every 30min. Confocal images of the window chamber were taken using a Leica SP5
479 confocal system with a 10.0x 0.30 N.A. objective. To be able to image the window chamber
480 mice were anesthetized with isoflurane. Due to the stressfulness of the anesthesia of the
481 imaging procedure, in vivo images were acquired every 2-3 days.
482 To precisely observe individual organoids, we took stacks of confocal images
483 (1024x1024 pixels, 41 images with a z- spacing of 0.25 microns) using a Leica SP5 confocal
484 microscope, with a 100x 1.43 N.A. oil immersion objective (Leica Microsystems) at a
485 resolution of 0.132 μm/pixel (image stacks were thus 135 mm * 135 mm * 10 mm). We
486 simultaneously collected the differential interference contrast (DIC) images as well as the
487 RFP- and GFP-signal.
488
489
490
491
492
493

494 **Acknowledgements:** We acknowledge technical assistance by Yaas Bigdeli and Ayse
495 Karakecili, and Mohammed Shaik and Elizabeth Hillman for help with imaging.
496
497 **Funding:** We acknowledge funding from NIH R01HL095477-05R01. N.S.R. was
498 supported by a fellowship from the Villum Foundation and Novo Nordisk Foundation
499 Visiting Scholar Fellowship at Stanford Bio-X (NNF15OC0015218. R.z.N. was
500 supported by the German National Academic Foundation, the Gerhard C. Starck
501 Foundation and the Klee Family Foundation.
502
503 **Author contributions:** N.S.R., R.z.N., B.M.G., and S.K.S. conceived the project and
504 designed the experiments. N.S.R., P.N.A., R.z.N., K.L., W.L., C.P., C.H., Q.F., Z.S.,
505 R.P.S.-M., J.C., J.E.G., N.S., T.H. and B.M.G. conducted the experiments and analyses.
506 N.S.R., P.N.A., R.z.N. and B.M.G. analyzed and interpreted the data. N.S.R., P.N.A.
507 and R.z.N. prepared the figures, and N.S.R., R.z.N., and S.K.S. wrote the manuscript
508 with contributions from P.N.A. and B.M.G.. N.S.R., B.M.G., P.N.A. and S.K.S.
509 supervised the project. All authors have reviewed the manuscript.
510
511 **Competing interests:** A patent has been filed by Columbia University on the technology
512 described in this study.

References

1 De Moor, L. *et al.* High-throughput fabrication of vascularized spheroids for bioprinting. *Biofabrication* **10**, 035009 (2018).

2 Wimmer, R. A. *et al.* Human blood vessel organoids as a model of diabetic vasculopathy. *Nature* **565**, 505-510 (2019).

3 McGuigan, A. P. & Sefton, M. V. Vascularized organoid engineered by modular assembly enables blood perfusion. *Proceedings of the National Academy of Sciences* **103**, 11461-11466 (2006).

4 Alajati, A. *et al.* Spheroid-based engineering of a human vasculature in mice. *Nat. Methods* **5**, 439-445, doi:10.1038/nmeth.1198 (2008).

5 Nam, K. H., Smith, A. S., Lone, S., Kwon, S. & Kim, D. H. Biomimetic 3D Tissue Models for Advanced High-Throughput Drug Screening. *Journal of Laboratory Automation* **20**, 201-215, doi:10.1177/2211068214557813 (2015).

6 Takebe, T. *et al.* Vascularized and functional human liver from an iPSC-derived organ bud transplant. *Nature* **499**, 481-484, doi:10.1038/nature12271 (2013).

7 Walser, R. *et al.* Generation of co-culture spheroids as vascularisation units for bone tissue engineering. *European cells & materials* **26**, 222-233 (2013).

8 Yap, K. K. *et al.* Enhanced liver progenitor cell survival and differentiation in vivo by spheroid implantation in a vascularized tissue engineering chamber. *Biomaterials* **34**, 3992-4001, doi:10.1016/j.biomaterials.2013.02.011 (2013).

9 Dissanayaka, W. L., Zhu, L., Hargreaves, K. M., Jin, L. & Zhang, C. Scaffold-free Prevascularized Microtissue Spheroids for Pulp Regeneration. *J. Dent. Res.* **93**, 1296-1303, doi:10.1177/0022034514550040 (2014).

10 Verseijden, F. *et al.* Prevascular structures promote vascularization in engineered human adipose tissue constructs upon implantation. *Cell Transplant.* **19**, 1007-1020, doi:10.3727/096368910X492571 (2010).

11 Meyer, U. *et al.* Cartilage defect regeneration by ex vivo engineered autologous microtissue--preliminary results. *In Vivo* **26**, 251-257 (2012).

12 Huch, M., Knoblich, J. A., Lutolf, M. P. & Martinez-Arias, A. The hope and the hype of organoid research. *Development* **144**, 938-941 (2017).

13 Sutherland, R. M., McCredie, J. A. & Inch, W. R. Growth of multicell spheroids in tissue culture as a model of nodular carcinomas. *J. Natl. Cancer Inst.* **46**, 113-120 (1971).

14 Tung, Y. C. *et al.* High-throughput 3D spheroid culture and drug testing using a 384 hanging drop array. *Analyst* **136**, 473-478, doi:10.1039/c0an00609b (2011).

15 Frey, O., Misun, P. M., Fluri, D. A., Hengstler, J. G. & Hierlemann, A. Reconfigurable microfluidic hanging drop network for multi-tissue interaction and analysis. *Nature Communications* **5**, 4250, doi:10.1038/ncomms5250 (2014).

16 Ehsan, S. M., Welch-Reardon, K. M., Waterman, M. L., Hughes, C. C. & George, S. C. A three-dimensional in vitro model of tumor cell intravasation. *Integr. Biol. (Camb.)* **6**, 603-610, doi:10.1039/c3ib40170g (2014).

17 Yuhas, J. M., Li, A. P., Martinez, A. O. & Ladman, A. J. A simplified method for production and growth of multicellular tumor spheroids. *Cancer Res.* **37**, 3639-3643 (1977).

18 Metzger, W. *et al.* The liquid overlay technique is the key to formation of co-culture spheroids consisting of primary osteoblasts, fibroblasts and endothelial cells. *Cytotherapy* **13**, 1000-1012, doi:10.3109/14653249.2011.583233 (2011).

19 Wenger, A. *et al.* Development and characterization of a spheroidal coculture model of endothelial cells and fibroblasts for improving angiogenesis in tissue engineering. *Cells Tissues Organs* **181**, 80-88, doi:10.1159/000091097 (2005).

20 Chung, H. J. & Park, T. G. Injectable cellular aggregates prepared from biodegradable porous microspheres for adipose tissue engineering. *Tissue Engineering Part A* **15**, 1391-1400, doi:10.1089/ten.tea.2008.0344 (2009).

21 Griffin, D. R., Weaver, W. M., Scumpia, P. O., Di Carlo, D. & Segura, T. Accelerated wound healing by injectable microporous gel scaffolds assembled from annealed building blocks. *Nat. Mat.* **14**, 737-744, doi:10.1038/nmat4294 (2015).

22 Huebsch, N. *et al.* Matrix elasticity of void-forming hydrogels controls transplanted-stem-cell-mediated bone formation. *Nat. Mat.* **14**, 1269-1277, doi:10.1038/nmat4407 (2015).

23 Li, Y. *et al.* Primed 3D injectable microniches enabling low-dosage cell therapy for critical limb ischemia. *Proceedings of the National Academy of Sciences* **111**, 13511-13516 (2014).

24 Ovsianikov, A., Khademhosseini, A. & Mironov, V. The synergy of scaffold-based and scaffold-free tissue engineering strategies. *Trends Biotechnol.* **36**, 348-357 (2018).

25 Li, N., Schwartz, M. & Ionescu-Zanetti, C. PDMS Compound Adsorption in Context. *J. Biomol. Screen.* **14**, 194-202, doi:10.1177/1087057106286653 (2009).

26 Toepke, M. W. & Beebe, D. J. PDMS absorption of small molecules and consequences in microfluidic applications. *Lab on a Chip* **6**, 1484-1486, doi:10.1039/b612140c (2006).

27 Shimizu, K. *et al.* Poly (N-isopropylacrylamide)-coated microwell arrays for construction and recovery of multicellular spheroids. *J. Biosci. Bioeng.* **115**, 695-699 (2013).

28 Tekin, H. *et al.* Stimuli-responsive microwells for formation and retrieval of cell aggregates. *Lab on a chip* **10**, 2411-2418 (2010).

29 Anada, T. *et al.* Three-dimensional cell culture device utilizing thin membrane deformation by decompression. *Sensors Actuators B: Chem.* **147**, 376-379 (2010).

30 Beebe, D. J. *et al.* Functional hydrogel structures for autonomous flow control inside microfluidic channels. *Nature* **404**, 588 (2000).

31 Gillette, B. M., Jensen, J. A., Wang, M., Tchao, J. & Sia, S. K. Dynamic hydrogels: switching of 3D microenvironments using two‐component naturally derived extracellular matrices. *Adv. Mater.* **22**, 686-691 (2010).

32 Zhao, X. *et al.* Active scaffolds for on-demand drug and cell delivery. *Proceedings of the National Academy of Sciences* **108**, 67-72 (2011).

33 Kusamori, K. *et al.* Transplantation of insulin-secreting multicellular spheroids for the treatment of type 1 diabetes in mice. *J. Control. Release* **173**, 119-124 (2014).

34 Lee, J., Sato, M., Kim, H. & Mochida, J. Transplantation of scaffold-free spheroids composed of synovium-derived cells and chondrocytes for the treatment of cartilage defects of the knee. *European Cells & Materials* **22**, 90 (2011).

35 Lee, J. M. *et al.* Generation of uniform-sized multicellular tumor spheroids using hydrogel microwells for advanced drug screening. *Sci. Rep.* **8**, 17145 (2018).

36 X Chen, Y., Cain, B. & Soman, P. Gelatin methacrylate-alginate hydrogel with tunable viscoelastic properties. *AIMS Materials Science* **4** (2017).

37 Gillette, B. M. *et al.* In situ collagen assembly for integrating microfabricated three-dimensional cell-seeded matrices. *Nat. Mat.* **7**, 636-640, doi:10.1038/nmat2203 (2008).

38 Gillette, B. M. *et al.* Engineering extracellular matrix structure in 3D multiphase tissues. *Biomaterials* **32**, 8067-8076, doi:10.1016/j.biomaterials.2011.05.043 (2011).

39 Lovett, M., Lee, K., Edwards, A. & Kaplan, D. L. Vascularization strategies for tissue engineering. *Tissue engineering. Part B, Reviews* **15**, 353-370, doi:10.1089/ten.teb.2009.0085 (2009).

40 Steffens, L., Wenger, A., Stark, G. B. & Finkenzeller, G. In vivo engineering of a human vasculature for bone tissue engineering applications. *J. Cell. Mol. Med.* **13**, 3380-3386, doi:10.1111/j.1582-4934.2008.00418.x (2009).

41 Miller, J. S. *et al.* Rapid casting of patterned vascular networks for perfusable engineered three-dimensional tissues. *Nat. Mat.* **11**, 768 (2012).

42 Bertassoni, L. E. *et al.* Hydrogel bioprinted microchannel networks for vascularization of tissue engineering constructs. *Lab on a Chip* **14**, 2202-2211 (2014).

43 Rouwkema, J. D. B., J.; Van Blitterswijk, C. A. Endothelial Cells Assemble into a 3-Dimensional Prevascular Network in a Bone Tissue Engineering Construct. *Tissue Eng.* **12**, 2685-2693 (2006).

44 Administration, F. a. D. Regulatory considerations for human cells, tissues, and cellular and tissue‐based products: Minimal manipulation and homologous use; guidance for industry and food and drug administration staff; availability. *Fed. Regist.* **82**, 54290-54292 (2017).

45 Fleming, P. A. *et al.* Fusion of uniluminal vascular spheroids: a model for assembly of blood vessels. *Dev. Dyn.* **239**, 398-406, doi:10.1002/dvdy.22161 (2010).

46 Mironov, V. *et al.* Organ printing: tissue spheroids as building blocks. *Biomaterials* **30**, 2164-2174, doi:10.1016/j.biomaterials.2008.12.084 (2009).

47 Huang, W. H. *et al.* Mesenchymal stem cells promote growth and angiogenesis of tumors in mice. *Oncogene* **32**, 4343-4354, doi:10.1038/onc.2012.458 (2013).

48 Iwase, T. *et al.* Comparison of angiogenic potency between mesenchymal stem cells and mononuclear cells in a rat model of hindlimb ischemia. *Cardiovasc. Res.* **66**, 543-551, doi:10.1016/j.cardiores.2005.02.006 (2005).

49 Davies, M. Critical limb ischemia: epidemiology. *Methodist Debakey Cardiovasc. J.* **8**, 10-14 (2012).

50 Tongers, J., Roncalli, J. G. & Losordo, D. W. Therapeutic angiogenesis for critical limb ischemia: microvascular therapies coming of age. *Circulation* **118**, 9-16, doi:10.1161/CIRCULATIONAHA.108.784371 (2008).

51 Raval, Z. & Losordo, D. W. Cell therapy of peripheral arterial disease: from experimental findings to clinical trials. *Circ. Res.* **112**, 1288-1302, doi:10.1161/CIRCRESAHA.113.300565 (2013).

52 Lawall, H., Bramlage, P. & Amann, B. Treatment of peripheral arterial disease using stem and progenitor cell therapy. *J. Vasc. Surg.* **53**, 445-453, doi:10.1016/j.jvs.2010.08.060 (2011).

53 Chen, L., Tredget, E. E., Wu, P. Y. & Wu, Y. Paracrine factors of mesenchymal stem cells recruit macrophages and endothelial lineage cells and enhance wound healing. *PLoS One* **3**, e1886, doi:10.1371/journal.pone.0001886 (2008).

54 Botham, C. M. B., W. L.; Cooke, J. P. Clinical trials of adult stem cell therapy for peripheral artery disease. *Methodist Debakey Cardiovasc. J.* **9** (2013).

55 Benoit, E., O'Donnell, T. F. & Patel, A. N. Safety and efficacy of autologous cell therapy in critical limb ischemia: a systematic review. *Cell Transplant.* **22**, 545-562, doi:10.3727/096368912X636777 (2013).

56 Laschke, M. W., Vollmar, B. & Menger, M. D. The dorsal skinfold chamber: window into the dynamic interaction of biomaterials with their surrounding host tissue. *European cells & materials* **22**, 147-164; discussion 164-147 (2011).

57 Palmer, G. M., Fontanella, A. N., Shan, S. & Dewhirst, M. W. High-resolution in vivo imaging of fluorescent proteins using window chamber models. *Methods Mol. Biol.* **872**, 31-50, doi:10.1007/978-1-61779-797-2_3 (2012).

FIGURES

Figure 1

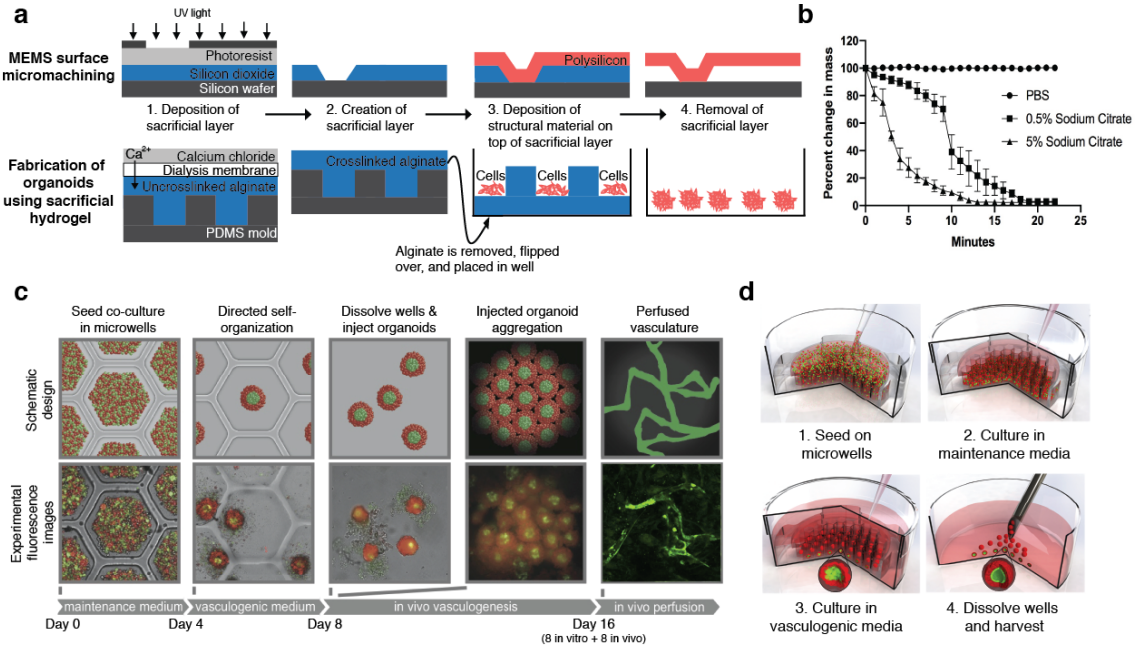

Fig. 1. Schematic diagram of method of using sacrificial hydrogels to produce therapeutic organoids. (A) Schematic demonstrating the parallels between the surface micromachining method to fabricate MEMS devices such as a microcantilever (top) and the use of sacrificial alginate microwells to fabricate organoids (bottom). Both methods involve the use of a sacrificial layer (blue) to fabricate the final structure (red). **(B)** Time required to completely uncrosslink alginate microwells following incubation with different concentrations of a chelator (sodium citrate) by measuring the percent change in mass over time (n=3, Error bars are standard deviations). **(C)** Schematic diagrams (top) and corresponding experimental images (bottom) showing the steps of organoid fabrication and *in vivo* perfusion. Experimental data were collected using GFP-labelled HUVECs and RFP-labelled mouse MSCs. First, a co-culture of endothelial cells (green) and therapeutic cells (red) is seeded on dissolvable alginate

683 microwells. Second, after being cultured in maintenance medium without growth
684 factors for 3 to 4 days, cells self-organize into organoids with an endothelial core. A
685 switch into culture medium with vasculogenic growth factors for an additional 4 days
686 promoted formation of vessels within the organoids. Third, alginate microwells were
687 dissolved with 5% sodium citrate to release organoids. Fourth, suspension of organoids
688 could be centrifuged and assembled into a macro-tissue *in vitro* to study vascular
689 formation, or injected into the subdermis or ischemic hindlimb of a mouse to
690 demonstrate engraftment *in vivo*. Fifth, injected organoids rapidly connected to form
691 perfused microvasculature *in vivo*. **(D)** The liquid handling steps in the process: 1)
692 seeding the co-culture of ECs (green) and MSCs (red) by pipetting cells onto alginate
693 microwell construct, 2) adding maintenance media once the cells have settled to the
694 bottom of the microwells (approx. 30 minutes), 3) switching to vasculogenic media
695 once an endothelial core has formed, and 4) gently dissolving the alginate microwells
696 (approx. 5 minutes) to harvest organoids (the organoids can be gently washed prior to
697 injection).
698
699

700 **Figure 2**

701

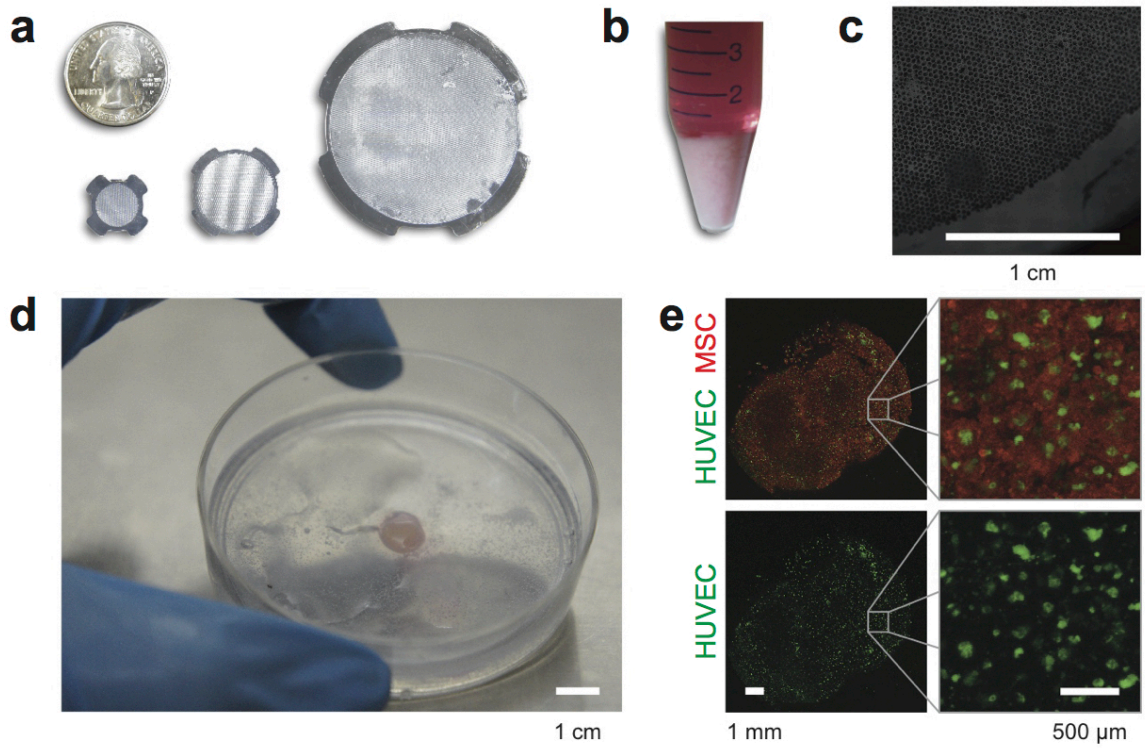

702

703 **Fig. 2. Production of organoids at large scale, and functionality of organoids to**
704 **form macrotissue. (A)** Pictures of three alginate microwells constructs for inserts into
705 24-well plates, 12-well plates or 60-mm dishes with the capacity to produce 24 × 1000,
706 12 × 3000 or 30,000 organoids respectively. **(B)** Picture of 250 million cells for
707 seeding into alginate microwells. Cells in this figure are GFP-labelled HUVECs and
708 RFP-labelled mouse MSCs. **(C)** Stitched brightfield image of cells seeded in a 60-mm
709 construct with 30,000 wells to create 30,000 organoids. Scale bar is 1 cm. **(D)** Picture
710 of a 1 mm thick macrotissues with an area of 1 cm^2 assembled *in vitro* by collecting the
711 30,000 mature pre-vascularized organoids produced with the alginate microwell (a and
712 b) construct in a 60-mm dish. Scale bar is 1 cm. **(E)** Fluorescence images of the
713 macrotissue in (d) with a close-up of the closely packed organoids with endothelial
714 cores (green). Scale bars are 1 mm (left) and 500 µm (right).

715

716 **Figure 3**

717

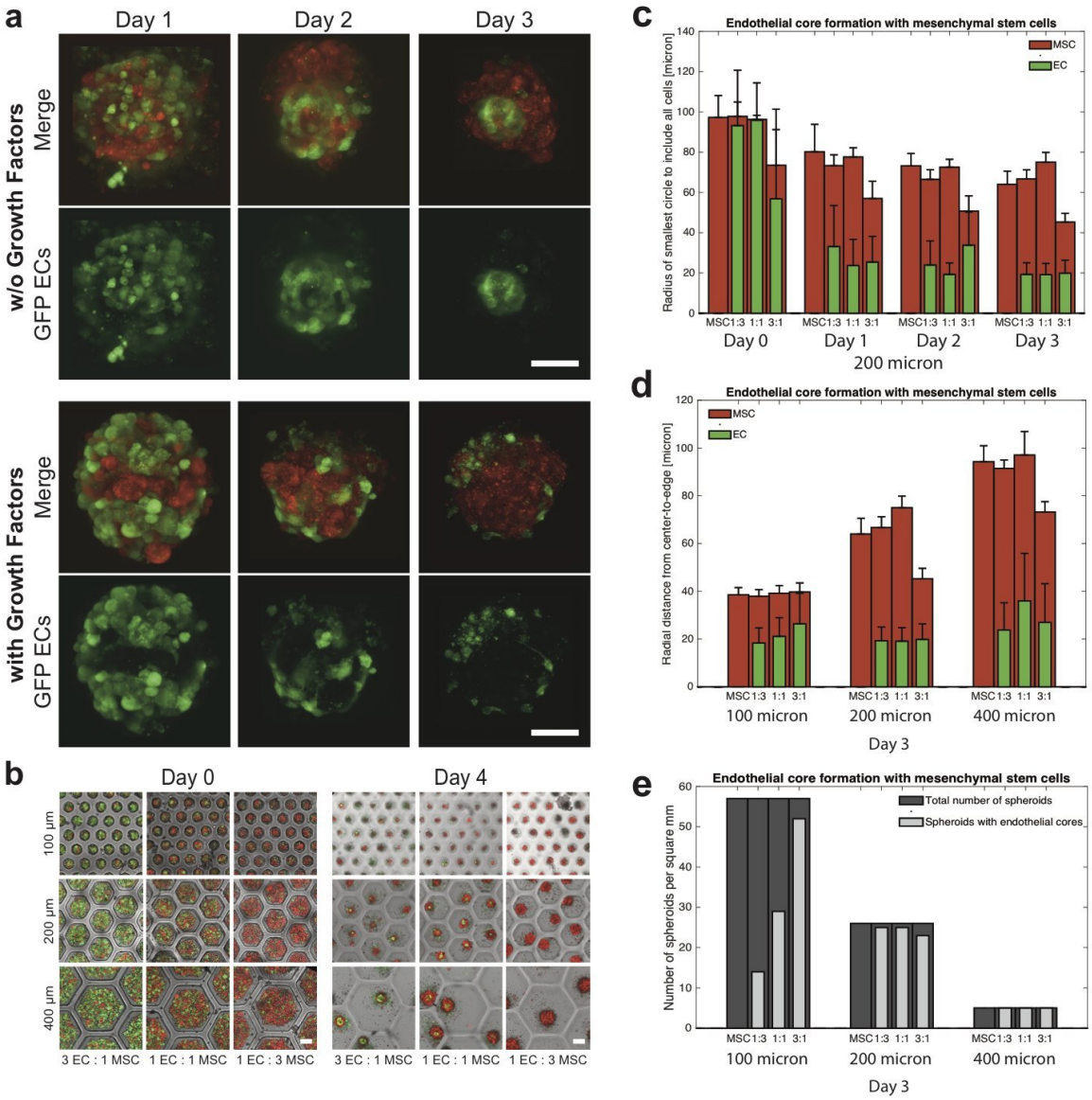

718

719 **Fig. 3. Production of vascularized organoids with high reproducibility in size and**

720 **structure. (A)** Confocal fluorescence images of co-culture organoids of GFP-labeled

721 HUVECs (green) and RFP-labeled mouse MSCs (red) over the first three days in

722 maintenance medium without growth factors (top) or in vasculogenic medium with 40

723 ng/mL VEGF and 40 ng/mL bFGF (bottom). The cells self-organize by migration, and

724 either formed endothelial cores when cultured in media without growth factors (top) or

725 had endothelial cells randomly distributed near the surface of the organoid and did not

726 form endothelial cores when cultured in media with growth factors (bottom). Scale
727 bars are 100 μm. **(B)** Overlay of fluorescent and transmitted images showing parallel
728 production of organoids in arrays of different sizes of microwells (with either 100, 200,
729 or 400 μm diameter) and different co-culture ratios (1 EC : 3 MSC, 1 EC : 1 MSC or 3
730 EC : 1 MSC). Different sizes of microwells yield different sizes of organoids, either
731 unvascularized with only MSCs or pre-vascularized with a co-culture of ECs and
732 MSCs, and different co-culture ratios yield different endothelial core sizes. Scale bars
733 are 100 μm. **(C)** Quantitative analysis of cell aggregation into organoids and the
734 formation of an endothelial core over time in 200 μm microwells, as measured by the
735 radius of the smallest circle that can contain all MSCs (red) or all ECs (green) ($n > 20$).
736 **(D)** Barplot showing the size of fully-contracted organoids (red) and the size of the
737 endothelial cores (green) for all tested microwell sizes and co-culture ratios. **(E)**
738 Reproducibility of endothelial cores; the number of organoids produced in 1 mm^2 (dark
739 grey) and the number of organoids containing and endothelial core (light grey) for all
740 tested microwell sizes and co-culture ratios.
741
742

743 **Figure 4**

744

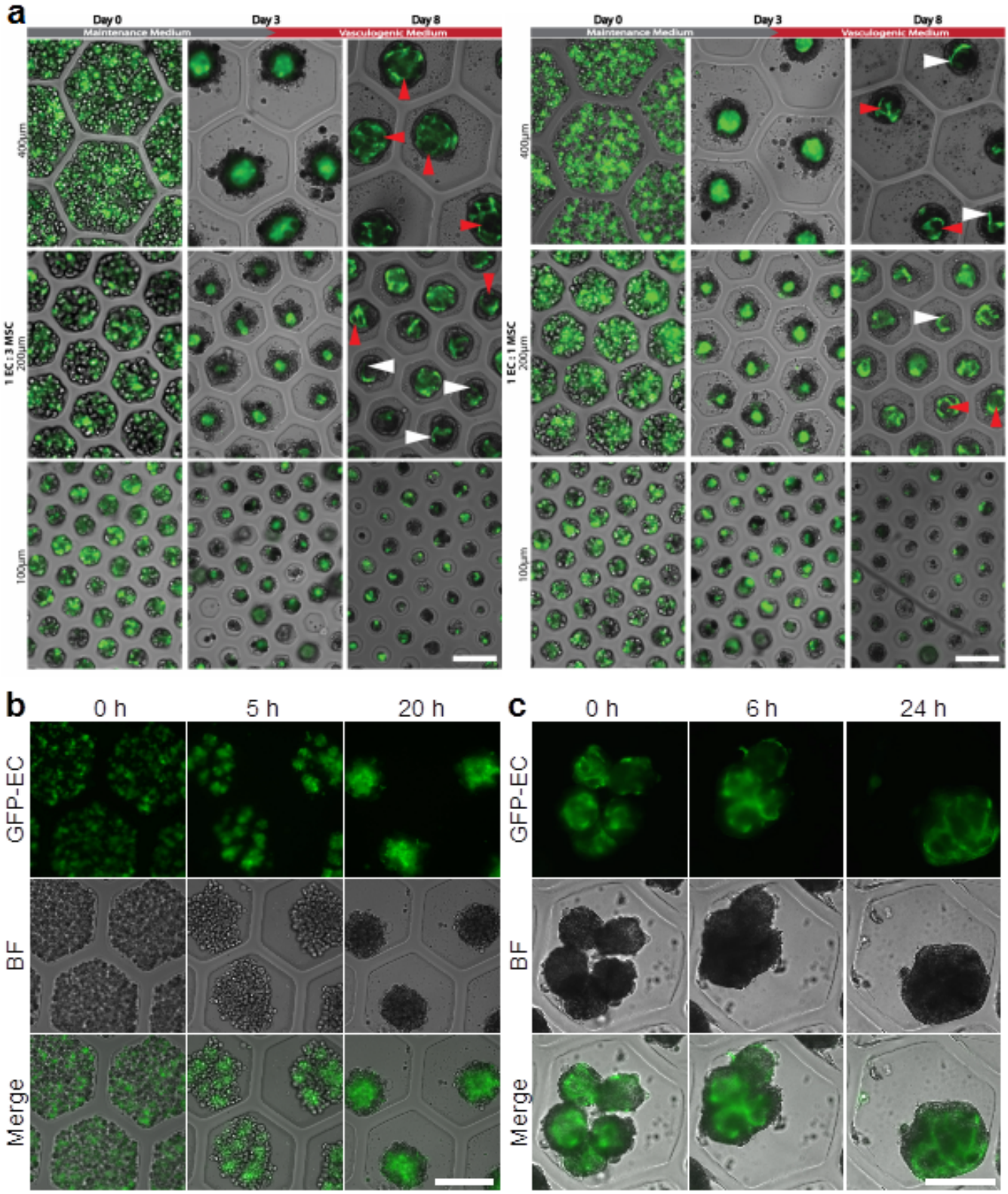

745

746

747 **Fig. 4. Production of vascularized organoids with human cells. (A)** Maturation of
748 endothelial cores with dynamic culture conditions for two co-culture ratios; 1 GFP-
749 HUVEC : 3 hAMSC (left) and 1 GFP-HUVEC : 1 hAMSC (right). The cells are seeded
750 (day 0) and initially cultured in maintenance medium without growth factors to form
751 endothelial cores. After 3 days the organoids were cultured in vasculogenic medium
752 with 40 ng/mL VEGF and 40 ng/mL bFGF and the endothelial cores matured into
753 vessels with discernable lumens (red arrows) and sprouts (white arrows). Scale bars are
754 200 μm. **(B)** Epifluorescence, brightfield, and overlay images showing early self-
755 organization of pre-vascularized organoids over the first 20 hours, with a 1 GFP-
756 HUVEC : 1 hAMSC co-culture in 400 μm microwells. Scale bar is 200 μm. **(C)**
757 Epifluorescence, brightfield, and overlay images showing fusion of pre-vascularized
758 organoids (same conditions as in right a and b) into mesotissues over the first 24 hours
759 of the fusion process within a 400 μm collagen-doped alginate microwell. Scale bar is
760 200 μm.
761

762 **Figure 5**

763

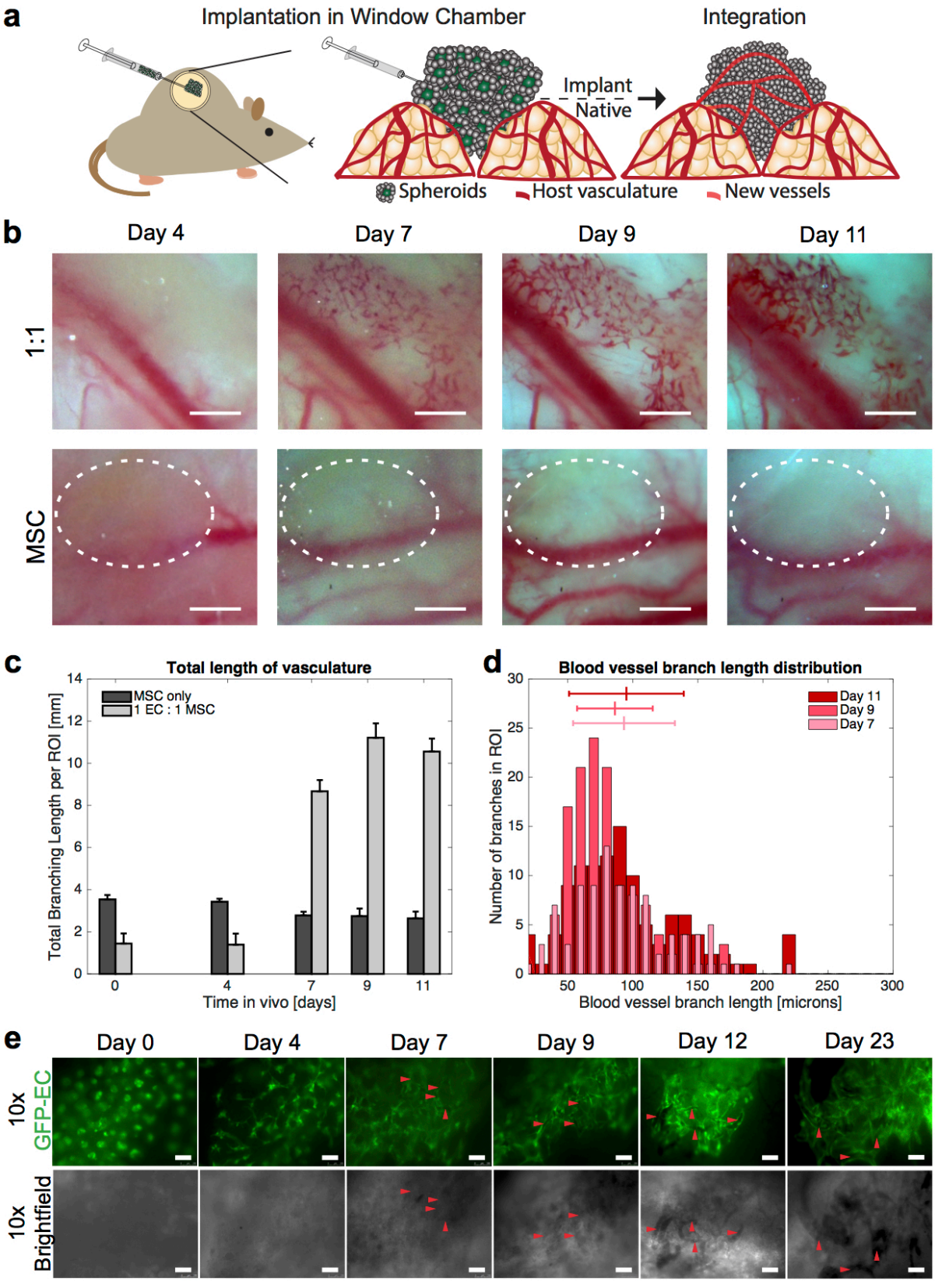

764

765 **Fig. 5. Rapid *in vivo* vascularization in healthy mice upon injection of organoids,**
766 **as observed in real time via a window chamber. (A)** Schematic diagram of
767 experimental setup for observing vascular formation and integration with host
768 vasculature *in vivo* in real time via a window chamber. Organoids (from human cells
769 formed under dynamic culture conditions in 200 μm microwells yielding organoids
770 71±5 μm in diameter) were injected into a window chamber implant in a SCID mouse.
771 **(B)** Real-time *in vivo* stereoscopic images of prevascularized microtisses with 1 GFP-
772 HUVEC : 1 hAMSC (top row) and unvascularized organoids with hAMSC only
773 (bottom row) through window chamber at different time points. Scale bars are 500 μm.
774 In the top row, newly formed vessels are apparent within 4 days, and blood-filled
775 vessels observed by day 7. In the bottom row, the dashed white line indicates the area
776 of organoids implant and no neo-vascularization was observed. **(C)** Quantification of
777 neo-vascularization of the prevascularized organoids as the total length of vasculature
778 within three ROI. The total length of vasculature increases substantially after day 7 for
779 prevascularized organoids. There is no substantial difference in total length of the
780 vasculature for the unvascularized organoids. **(D)** Histograms of branching length in
781 the newly formed microvasculature (b and c) at day 7, 9 and 11. Lines above histogram
782 indicate the mean branch length and standard deviation for day 7, day 9, and day 11 as
783 93 ± 39 μm, 86 ± 29 μm, and 93 ± 44 μm respectively. **(E)** Real-time *in vivo* images of
784 prevascularized organoids with endothelial cells in green. Red arrow heads point to
785 luminous, blood-filled vessels (as indicated by dark lines in fluorescence images and
786 dark areas of brightfield images). Scale bar is 250 μm.
787
788